A NEW DEFECTED GROUND STRUCTURE AND ITS APPLICATION FOR MINIATURIZED SWITCHABLE ANTENNA

J. X. Liu, W. Y. Yin, and S. L. He [†]

Center for Optical and Electromagnetic Research
State Key Lab of MOI
Zhejiang University
Hangzhou 310058, China

Abstract—A new defected ground structure (DGS) is firstly proposed in this paper, which has better slow-wave effect than that of cross or dumbbell one. Using the model of transmission line, its equivalent parameters are extracted. With good omni-directional properties, the proposed DGS is then used in the design of a proximity coupled antenna for its miniaturization. The size of the developed antenna is about 68% smaller than that of the conventional one. Further, two artificial cells are added on the feed line to reduce the protrudent stub length from 26.9 mm to 18.94 mm. With the utility of the DGS and artificial cells, the size of proximity coupled antenna is reduced significantly. By introducing a PIN diode at the end of feed line, the antenna is switchable in both x- and y-direction linear polarizations. Such miniaturization in antenna size has little negative effect on its cross polarization, with both simulated and experimental results presented for comparison.

1. INTRODUCTION

With the rapid development of wireless communication, much effort has been devoted to reducing the size of microstrip antenna, with a lot of methods proposed recently, such as cutting slots on the patch, meandering the lateral edge of patch, using stacked patch, and adopting the substrate with high permittivity, etc. [1–9]. Moreover, some structures are etched in the patch or ground plane to miniaturize

the size of antenna [10–14]. This method utilizes the slower phase velocity in the etched devices than that in conventional ones.

Defected ground structure (DGS) is a convenient way to realize the slow wave effect. It has been widely used in the development of miniaturized antennas [15–18]. Many DGS patterns are studied so as to improve their performance. In [19], dog bone structure is used as defected ground, and in [20], one spiral DGS is chosen for size miniaturization. More recently, many modified patterns, such as H-, U- and T-shaped DGSs are presented for achieving high Q-factor [21–24].

When the DGSs are used in the design of antennas, cross shape may be required for good radiation patterns or polarizations. A conventional cross shaped DGS is proposed in [25] for compact circular polarization antenna. In [26], a cross dumbbell shaped DGS is introduced. However, it is found that their slow-wave factors (SWFs) are not satisfied, with large resonant loss produced. Here, a new DGS will be proposed for improved slow wave effect and unloaded Q-factor.

On the other hand, in order to reduce the length of transmission line, some planar artificial cells are introduced in [27, 28], which are compact in size and easy to be fabricated using standard printed circuit board (PCB) technology. The planar artificial cells have quasi-lumped structures, with no use for extra surface mounted devices or via holes.

Modern wireless communication is facing with another challenge of frequency reuse. Polarization reconfigurable antennas can provide different polarizations at one frequency. Varactors, PIN diodes and even MEMS switches can be used as control components. A conventional proximity coupled antenna has been designed for switchable polarization with the advantage of little DC interference on the patch. The cross polarization levels are $-14\,\text{dB}$ for the OFF state, and $-10.2\,\text{dB}$ for the ON state at $2.8\,\text{GHz}$ [29]. However, the conventional square patch occupies a large area, and the antenna has not satisfied return loss at the ON state.

In this paper, a miniaturized proximity coupled antenna with DGS is developed for switchable polarization application. The organization of this paper is as follows. In Section 2, a new DGS is proposed, and compared with the conventional cross and dumbbell shaped ones, the proposed DGS has better SWF and higher unloaded Q-factor. Related parameters are analyzed to study their effects on the slow wave factor. In Section 3, a DGS etched proximity coupled antenna is presented, and two artificial transmission line cells are inserted in the feed line to further reduce the antenna occupancy. A PIN diode is soldered as one part of the proposed miniaturized antenna so as to achieve polarization reconfigurability. It is shown that these improvements

can reduce the antenna size greatly, but with little degradation in its cross polarization. Some conclusions are finally drawn in Section 4.

2. DEFECTED GROUND STRUCTURE (DGS)

2.1. Slow Wave Factor of the Cross, Dumbbell and Proposed DGSs

As shown in Figure 1(a), cross shaped DGS is usually used in the design of a compact antenna. However, it has low unloaded Q-factor and high transmission loss. To improve its performance, a dumbbell shaped DGS is introduced in Figure 1(b). In Figure 1(c), a DGS with four connecting E-shaped slots is proposed to improve the Q-factor with small occupancy. These DGSs are simulated and compared with the help of Ansoft HFSS software. In the simulation, the substrate has the permittivity of 2.65 and the thickness of 1 mm. A 50 Ω transmission line with the width of 2.8 mm is printed on one side of substrate, with a DGS etched on the ground of the other side.

Such three types of DGSs have the same length and width, i.e., $L = 23.16$ mm, $w = 2.87$ mm, and $w_1 = 0.615$ mm. To compare the slow wave effect with different slot widths, a wide cross shaped DGS with $w_1 = 2.87$ mm is also simulated. The S_{21} parameters of various DGSs are plotted in Figure 2.

It is shown that, the wide cross DGS has a higher resonant frequency than that of the narrower one. The dumbbell DGS has a lower frequency than that of the narrower cross one. So, for a fixed stop band frequency (SBF), the size of dumbbell DGS is smaller than that of cross one. The proposed DGS has the lowest resonant frequency
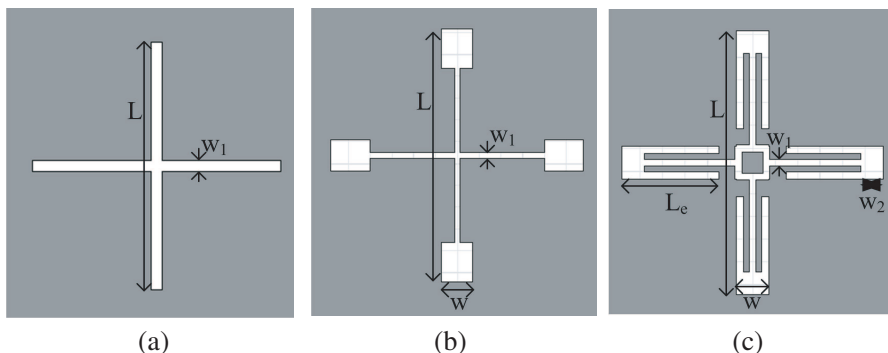

Figure 1. Geometries of three types of DGSs: (a) cross; (b) dumbbell; and (c) the proposed shape.
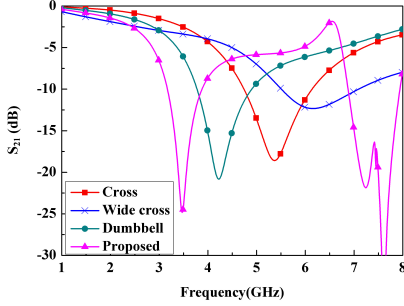
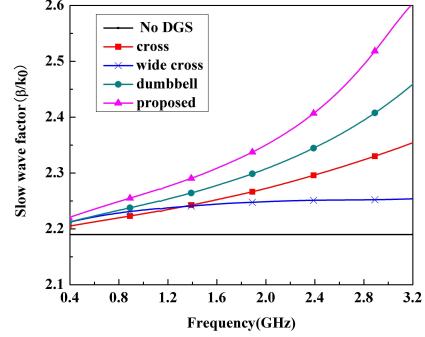**Figure 2.** Transfer characteristics for different DGSs.

Figure 3. SWF as a function of frequency for different DGSs.

of 3.47 GHz among these DGSs. The SWFs of the DGSs are calculated by [19]:

$$\beta/k_0 = \sqrt{\epsilon_{eff,d}} = \lambda_0 \Delta\theta/(360L) + \sqrt{\epsilon_{eff}} \qquad (1)$$

where $\epsilon_{eff,d}$ is the effective permittivity of the substrate with DGS etched ground plane, λ_0 is the wavelength in free space, $\Delta\theta$ is the phase difference between the microstrip line with and without DGS, L is the length of $50\,\Omega$ microstrip line, and ϵ_{eff} is the effective permittivity but with no DGS included.

Slow wave effect occurs only when the operating frequency is lower than the SBF of the DGS. Therefore, only the SWFs in the frequency band of 0.4–3.2 GHz are shown in Figure 3, and with no DGS implemented, the SWF is 2.19 at 2.25 GHz. In comparison, the SWFs for wide cross, narrow cross, dumbbell and proposed DGSs are equal to 2.25, 2.287, 2.33, and 2.384, respectively. So, the wide cross DGS has the lowest SWF among all these DGSs. For its worst slow wave effect, the wide cross one will be excluded in further study. On the other hand, compared with cross and dumbbell ones, the proposed DGS has the largest slope in the slow wave region.

2.2. Unloaded Q-factor of the DGSs

To extract the Q-factors of the DGSs, three DGS samples are redesigned with the same SBF at 3.47 GHz, and their S-parameters are plotted in Figure 4. The narrowest bandwidth of the proposed one means its best stop band sensitivity. As shown in the second row of Table 1, the length of the proposed DGS is 23.165 mm, which is 64% of the cross DGS and 81% of the dumbbell one in size, respectively. The narrowest slit is still set to be $w_1 = 0.615$ mm.
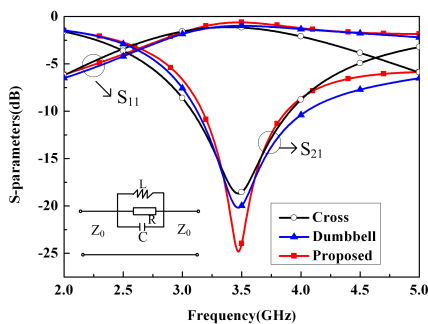
Figure 4. S-parameters for different DGSs with the same SBF.

Table 1. Extracted parameters of different DGSs.

DGS	Size $(\text{mm} \times \text{mm})$	f_c (GHz)	C (pF)	L (nH)	R (Ω)	Q
Cross	35.74×0.615	2.342	0.5686	3.7	681.25	8.445
Dumbbell	28.66×2.87	2.495	0.6828	3.08	771.08	11.478
Proposed	23.165×2.87	2.5789	0.7615	2.76	1289	21.398

The simplified equivalent circuit model of DGS is made of a shunt connection of a resistor, a capacitor and an inductor, as shown in the inset of Figure 4. The extracted element parameters are summarized in Table 1, with [23]

$$C = \omega_c / \left[2Z_0 \left(\omega_0^2 - \omega_c^2 \right) \right], \quad L = 1/\omega_0^2 C, \tag{2}$$

$$R = \frac{2Z_0}{\sqrt{1/ \left(|S_{11}(\omega_0)|^2 \right) - \left[2Z_0 \left(\omega_0 C - 1/ \left(\omega_0 L \right) \right) \right]^2 - 1}} \tag{3}$$

where ω_0 is the center stop band angular frequency, ω_c is the 3 dB cutoff angular frequency, Z_0 is the characteristic impedance of transmission line, $S_{11}(\omega_0)$ is the magnitude of the simulated reflection coefficient at SBF. The unloaded Q-factor of each DGS is calculated by $Q = \omega_0 RC$.

It is known that the unloaded Q-factor of DGS is proportional to $\sqrt{C/L}$ [23]. In Table 1, from cross shaped DGS to the proposed one, the capacitance is increased while the inductance is decreased, which leads to a continuous improvement in its Q-factor. It is more than 2.5 times of the cross shaped one, with very low transmission loss produced.
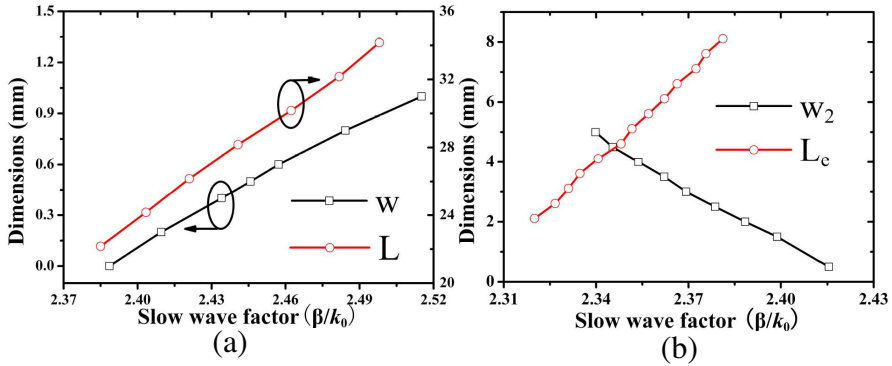
Figure 5. DGS dimensions as a function of slow wave factor.

2.3. Effect of the Dimensions

For the proposed DGS, the effects of the dimensions, the DGS length L, the width w, the branch length L_e and the margin width w_2 on the slow wave performance of the DGS are simulated and presented in Figure 5. Compared with the length L, the SWF is more sensitive to the slight changes of width w. The width w_2 is inverse proportional to the SWF. This is because the proposed DGS will gradually turn to a conventional cross shape when w_2 is increasing. Therefore, large SWF can be gained with narrower w_2. Additionally, longer L_e can also increase the SWF so that the size of microwave device is reduced.

3. PROXIMITY COUPLED ANTENNA WITH SWITCHABLE POLARIZATION

3.1. DGS Etched Proximity Couple-fed Antenna

As miniaturizing the size of the proximity coupled antenna, the modification on patch will probably deteriorate its cross polarization or impedance matching. To solve this problem, the slow-wave characteristics of the DGSs are utilized to reduce the resonant frequency of antenna. The DGSs are etched on the ground plane under the patch center. A proximity coupled antenna with the proposed DGS is illustrated in Figure 6. Its square patch has a lateral size of 24.54 mm, and the DGSs have the same size as that in Figure 2. Without the DGS, the antenna resonates at 3.63 GHz. The simulated reflection coefficients with various DGSs are plotted in Figure 7. Corresponding to Figure 3, the antenna with cross shaped DGS shows the worst slow-wave effect and resonates at 2.42 GHz, while the proposed DGS
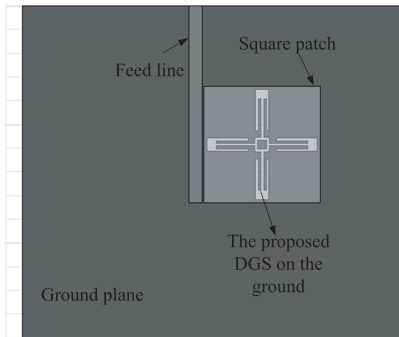
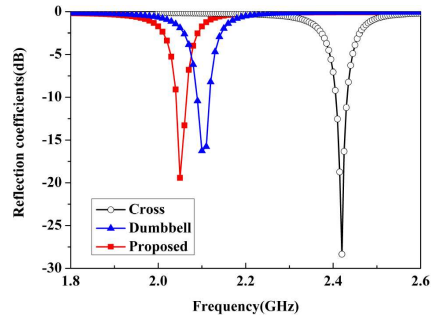**Figure 6.** Proximity coupled antenna with the proposed DGS.

Figure 7. Reflection coefficients for different DGSs.

resonates at 2.05 GHz. In other words, the proposed DGS etched antenna has a size reduction of $1 - (2.05/3.63)^2 = 68\%$ than that of the conventional proximity coupled one.

3.2. Artificial Cells Etched on the Feed Line

To further reduce the size of antenna, the artificial structures are utilized to shorten the length of the feed line. Figure 8 shows the transmission phase shifts with different numbers of artificial transmission cells. The inset illustrates the simulated model of the transmission line with two artificial cells implemented. For the same line with length of 18.94 mm and width of 1.5 mm, the phase shift has about $30°$ improvement when two cells are used. For instance, the conventional transmission line has a phase shift of $75°$ at 2.25 GHz. The phase shift becomes $106.4°$ when two cells are inserted with an insertion loss of 0.133 dB. For the same phase shift of $106.4°$, the conventional line requires 26.9 mm in length, which is about 8 mm longer than that of the transmission line with two cells inserted. More artificial cells can be inserted for further reduction of the line length. As a matter of fact, the transmission line with three cells etched has a phase shift of $121°$ with the transmission line of 15 mm in length. However, only two cells are used here so as to save enough space for soldering the PIN diode.

3.3. Polarization Switchable Antenna

The proposed antenna in Figure 6 is used to design polarization switchable antenna operating at two different linear polarizations along
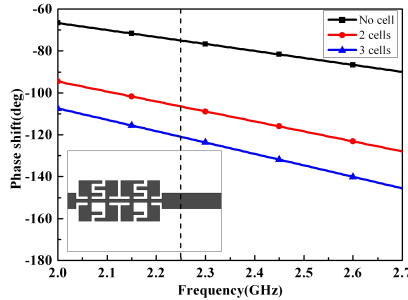
Figure 8. Phase shift as a function of frequency for different numbers of artificial cells.
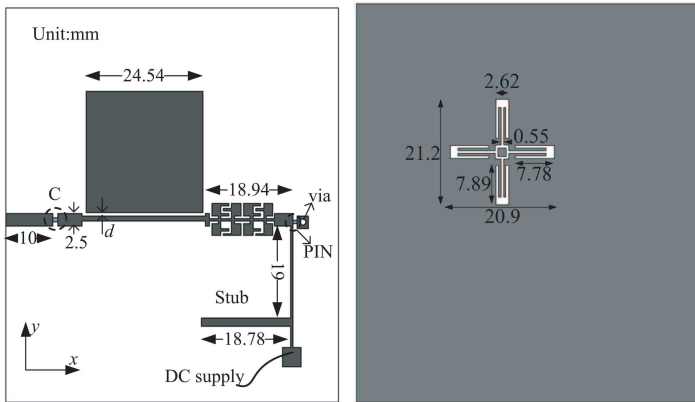

Figure 9. Geometry of the proposed switchable antenna.

the x- and y-direction, respectively. Its structure and biasing circuit are depicted in Figure 9. The total length of feed line is 58.75 mm. Two artificial cells are inserted in the protrudent feed line. The PIN diode is soldered between the terminal of the feed line and the 2.5 mm × 2.5 mm pad with a ground via. By Switching the PIN diode ON or OFF, the feed line terminal is shorted or opened to the ground, corresponding to the change of the linear polarization from x- to y-direction, respectively. A 5 pF capacitor is inserted at a position of 10 mm away from the feed point to isolate DC current. A $\lambda/4$ length stub of 18.78 mm is used as AC block. The distance d between the feed line and the patch is tuned to optimize the impedance matching. With smaller d, the impedance at the OFF state is matched better, and here $d = 0.2$ mm is chosen in the design.

When the diode is switched on, the feed line is inductively coupled with the radiation patch, so an electric current along x-axis is produced. Instead, when the diode is switched off, the feed line is capacitively coupled with the radiation patch, and the current flows along the y-axis. To enhance capacitive coupling, the feed line width is chosen to be 2.5 mm. The width is further reduced to 0.75 mm for the segment of feed line below the radiation patch.

In the design, an Infineon Bar63-02V PIN diode is used to switch the two linear polarizations. In the simulation, the diode is replaced by a 2 Ω resistor at the ON state, and represented by the shunt connection of a 5 kΩ resistor and a 0.3 pF capacitor at the OFF state. For fine-tuning of the impedance matching and cross polarization, the two crossed DGS components are set with little difference, which are 21.2 and 20.9 mm in length, respectively.

The simulated and measured reflection coefficients are shown in Figure 10. The simulated resonant frequencies at the ON and OFF states are equal to 2.23 and 2.25 GHz, respectively. The measured reflection coefficients agree well with the simulated ones. The antenna has good impedance matching for −10 dB specification.

The simulated and measured radiation patterns at the two states are shown in Figures 11 and 12, respectively. At the ON state, the antenna has an eight-shape pattern on the x-z plane and omni-directional pattern on the y-z plane. Opposite radiation patterns are observed at the OFF state. The large back lobe is caused by the energy leakage from the DGS on the ground plane, which can be suppressed by adding a metal reflector with one quarter wavelength distance from the antenna.
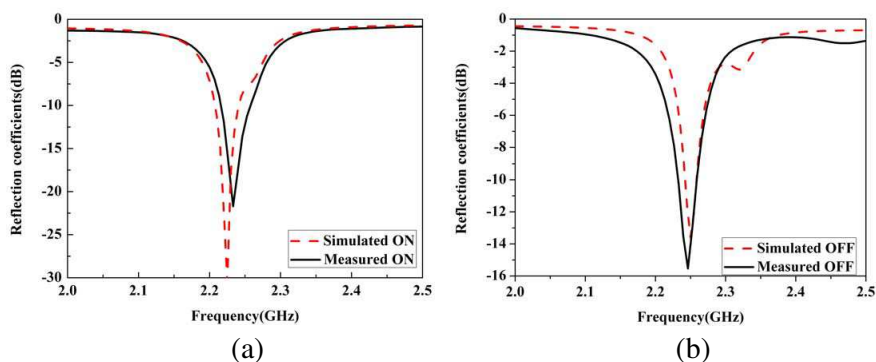

Figure 10. Measured and simulated reflection coefficients in (a) ON; and (b) OFF states, respectively.
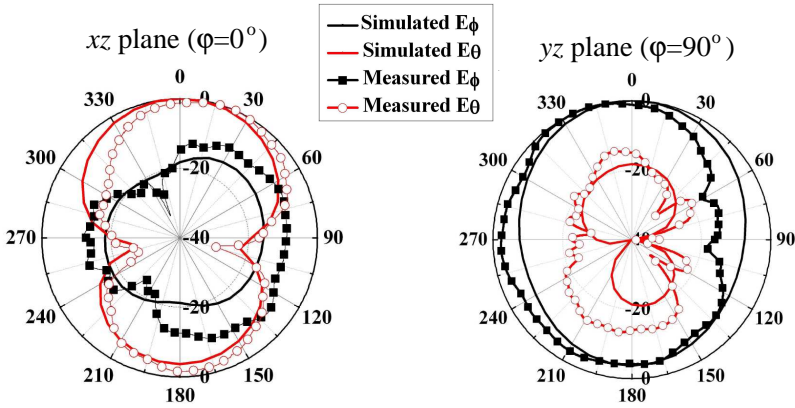
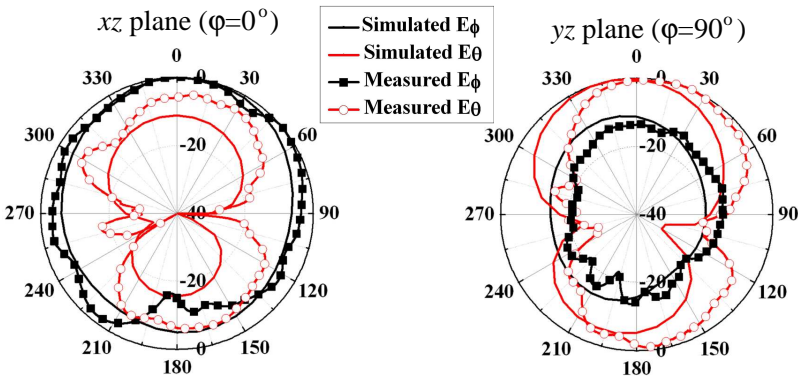**Figure 11.** Radiation patterns at the ON state of the developed antenna.

Figure 12. Radiation patterns at the OFF state of the developed antenna.

To take both co- and cross- polarization into account, $\varphi = 0°$ plane is chosen as an example. When the diode is switched on, the current flows along the x-direction, E_θ is the main polarization component, while the cross polarization E_φ-component is below -18 and -15 dB in the simulation and measurement, respectively. When the PIN diode is tuned to OFF state, the cross polarization level is -10 and -6 dB in the simulation and measurement, respectively. The cross polarization at the OFF state is worse than that of the ON state, which maybe caused by the sensitively capacitive coupling between the feed line and the patch. The measured cross polarization level is 3–4 dB lower than that of the simulated ones. The discrepancy may be caused by the parasitic effects of diode package, which are not taken into account

in the simulation. The simulated and measured gain is 3.8 dB and 2.8 dB at the ON state, and 3.74 dB and 2.5 dB at the OFF state, respectively. The simulated efficiency is 77% and 79% at ON and OFF state, respectively.

4. CONCLUSION

A new DGS structure with good slow wave effect is presented in this paper. Its characteristics are compared with conventional cross shaped and dumbbell ones, respectively. Based on the equivalent parameters extracted from full-wave simulation, the proposed DGS presents higher Q-factor and lower resonant loss than that of cross and dumbbell DGSs. With the same size, it has the lowest resonant frequency, which makes the structure more compact than that of the other DGSs. By introducing the proposed DGS in the proximity coupled antenna, the patch size, as compared with the conventional one, is reduced by 68%. Moreover, the introduction of two artificial transmission line cells shortens the length of the protrudent feed line from 26.9 mm to 18.94 mm. The miniaturized proximity coupled antenna is further used to realize switchable polarization. By switching on the PIN diode between the end of feed line and the ground plane, the antenna can resonate at x-direction polarization. On the other hand, if the diode is switched off, the polarization of the radiation field is turned into y-direction. In a word, with the proposed DGS, the polarization switchable antenna is miniaturized significantly, with an acceptable cross polarization at each state. The developed antenna can be a good candidate for the application of wireless communication.

ACKNOWLEDGMENT

REFERENCES

1. Heidari, A. A., M. Heyrani, and M. Nakhkash, "A dual-band circularly polarized stub loaded microstrip patch antenna for GPS applications," *Progress In Electromagnetics Research*, Vol. 92, 195–208, 2009.

2. Yang, X. D., Y. S. Li, and C. Y. Liu, "A toothbrush-shaped patch antenna for millimeter-wave communication," *Journal of*

Electromagnetic Waves and Applications, Vol. 23, No. 1, 31–37, 2009.

3. Li, J.-F., B.-H. Sun, H.-J. Zhou, and Q.-Z. Liu, "Miniaturized circularly-polarized antenna using tapered meander-line structure," *Progress In Electromagnetics Research*, Vol. 78, 321–328, 2008.

4. Wi, S. H., Y. B. Sun, I. S. Song, S. H. Choa, I. S. Koh, Y. S. Lee, and J. G. Yook, "Package-level integrated antennas based on LTCC technology," *IEEE Trans. Antennas Propag.*, Vol. 54, No. 8, 2190–2197, 2006.

5. Krishna, D. D., M. Gopikrishna, C. K. Aanandan, P. Mohanan, and K. Vasudevan, "Compact dual band slot loaded circular microstrip antenna with a superstrate," *Progress In Electromagnetics Research*, Vol. 83, 245–255, 2008.

6. Zhao, G., F. S. Zhang, Y. Song, Z. B. Weng, and Y. C. Jiao, "Compact ring monopole antenna with double meander lines for 2.4/5 GHz dual-band operation," *Progress In Electromagnetics Research*, Vol. 72, 187–194, 2007.

7. Zhang, Z.-Y., G. Fu, and S.-L. Zuo, "A miniature sleeve meander antenna for TPMS application," *Journal of Electromagnetic Waves and Applications*, Vol. 23, No. 14–15, 1835–1842, 2009.

8. Geyi, W., Q. Rao, S. Ali, and D. Wang, "Handset antenna design: Practice and theory," *Progress In Electromagnetics Research*, Vol. 80, 123–160, 2008.

9. Liu, W. C., S. H. Chen, and C. M. Wu, "Implantable broadband circular stacked PIFA antenna for biotelemetry communication," *Journal of Electromagnetic Waves and Applications*, Vol. 22, No. 13, 1791–1800, 2008.

10. Fontgalland, G., P. I. L. Ferreira, T. P. Vuong, N. Raveu, and H. Baudrand, "Proposal of new EBG ground planes in the electric size reduction design of planar antennas," *IEEE Advanced Industrial Conf. Telecom.*, 274–278, 2005.

11. Ramadan, A. H., K. Y. Kabalan, A. El-Hajj, S. Khoury, and M. Al-Husseini, "A reconfigurable U-koch microstrip antenna for wireless applications," *Progress In Electromagnetics Research*, Vol. 93, 355–367, 2009.

12. Kim, S. H., K. H. Oh, H. Lim, J. I. Song, and J. H. Jang, "Slow-wave characteristics of a 1D EBG structure for a miniaturized monopole antenna," *Microwave. Opt. Technol. Lett.*, Vol. 51, No. 5, 1231–1235, 2009.

13. Kordzadeh, A. and F. Hojat Kashani, "A new reduced size

microstrip patch antenna with fractal shaped defects," *Progress In Electromagnetics Research B*, Vol. 11, 29–37, 2009.

14. Hosseini, S. A., Z. Atlasbaf, and K. Forooraghi, "Two new loaded compact planar ultra-wideband antennas using defected ground structures," *Progress In Electromagnetics Research B*, Vol. 2, 165–176, 2008.

15. Kim, J. H, I. K. Kim, J. G. Yook, and H. K. Park, "A slow-wave structure with Koch fractal slot loops," *Microwave Opt. Technol. Lett.*, Vol. 34, No. 2, 87–88, 2002.

16. Tang, I. T., D. B. Lin, and T. H. Lu, "Applying the slow-wave effect in the design of a compact antenna," *Microwave Journal*, Vol. 51, No. 6, 96–96, 2008.

17. Fries, M. K. and R. Vahldieck, "Small microstrip patch antenna using slow-wave structure," *IEEE Antennas Propag. Society International Symposium*, Vol. 1–4, 770–773, 2000.

18. Geng, J.-P., J. Li, R.-H. Jin, S. Ye, X. Liang, and M. Li, "The development of curved microstrip antenna with defected ground structure," *Progress In Electromagnetics Research*, Vol. 98, 53–73, 2009.

19. Liu, H., Z. Li, and X. Sun, "Compact defected ground structure in microstrip technology," *Electron. Lett.*, Vol. 41, No. 3, 132–134, 2005.

20. Lim, J. S., C. S. Kim, Y. T. Lee, D. Ahn, and S. Nam, "A spiral-shaped defected ground structure for coplanar waveguide," *IEEE Microwave Wireless Comp. Lett.*, Vol. 12, No. 9, 330–332, 2002.

21. Kim, H. M. and B. Lee, "Bandgap and slow/fast-wave characteristics of defected ground structures (DGSs) including left-handed features," *IEEE Trans. Microwave Theory Techn.*, Vol. 54, No. 7, 3113–3120, 2006.

22. Woo, D. J., T. K. Lee, J. W. Lee, C. S. Pyo, and W. K. Choi, "Novel U-slot and V-slot DGSs for bandstop filter with improved Q factor," *IEEE Trans. Microwave Theory Tech.*, Vol. 54, No. 6, 2840–2847, 2006.

23. Huang, S. Y. and Y. H. Lee, "A compact E-shaped patterned ground structure and its applications to tunable bandstop resonator," *IEEE Trans. Microwave Theory Tech.*, Vol. 57, No. 3, 657–666, 2009.

24. Weng, L. H., Y.-C. Guo, X.-W. Shi, and X.-Q. Chen, "An overview on defected ground structure," *Progress In Electromagnetics Research B*, Vol. 7, 173–189, 2008.

25. Bao, X. L. and M. J. Ammann, "Dual-frequency circularly-

       polarized patch antenna with compact size and small frequency ratio," *IEEE Trans. Antennas Propag.*, Vol. 55, No. 7, 2104–2107, 2007.

26. Oskouei, H. D., K. Forooraghi, and M. Hakkak, "Guided and leaky wave characteristics of periodic defected ground structures," *Progress In Electromagnetics Research*, Vol. 73, 15–27, 2007.

27. Wang, C. W., T. G. Ma, and C. F. Yang, "A new planar artificial transmission line and its applications to a miniaturized butler matrix," *IEEE Trans. Microwave Theory Tech.*, Vol. 55, No. 12, 2792–2801, 2007.

28. Ma, T. G., C. W. Wang, R. C. Hua, and J. W. Tsai, "A modified Quasi-Yagi antenna with a new compact microstrip-to-coplanar strip transition using artificial transmission lines," *IEEE Trans. Antennas Propag.*, Vol. 57, No. 8, 2469–2474, 2009.

29. Tokunaga, I., M. Yamamoto, I. Nojima, and K. Itoh, "Polarisation switchable microstrip array antenna using proximity feeding technique," *Electron. Lett.*, Vol. 39, No. 22, 1569–1570, 2003.